Journal of Engineering Mathematics manuscript No.
(will be inserted by the editor)

A note on quasiperiodic Green's functions for arrays

Rachel I Brougham · **Ian Thompson**

Received: date / Accepted: date

Abstract We consider a one-dimensional array in two-dimensional space (a grating), and obtain a new representation for the associated quasiperiodic Green's function for the Helmholtz equation, intended for use when the observer is on, or close to, the axis of the array. This is compared to a formula from existing literature, which was obtained using Ewald summation. We find that the new representation is easier to compute, and generalises to account for arrays of higher order singularities in a simple way.

Keywords Quasiperiodic Green's function · gratings · arrays · lattices

1 Introduction

Quasiperiodic Green's functions (QPGs) for the Helmholtz equation are used extensively in modelling wave interactions with lattices and arrays. This dates back at least as far as [22], where QPGs are used (without being named as such) in determining the scattered field induced by a plane electromagnetic wave impinging upon a periodic grating. Recently, QPGs have been used in modelling interactions of water waves with ices floes [4], acoustic wave scattering by the ocean surface [1], electromagnetic wave propagation through photonic crystals [3], and flexural wave scattering by arrays of pins in thin elastic plates [21]. QPGs were also used in proving the existence of trapped modes in waveguides [8], and they play a central role in calculating the proportion of energy that is converted into Bloch waves when a field incident from outside strikes a periodic medium [23].

Rachel I Brougham
Department of Mathematical Sciences, University of Liverpool, Liverpool L69 7ZL, UK
E-mail: R.I.Brougham@liverpool.ac.uk

Ian Thompson
Department of Mathematical Sciences, University of Liverpool, Liverpool L69 7ZL, UK
E-mail: ian.thompson@liv.ac.uk

The fundamental (or spatial) representation for a QPG is constructed by adding together contributions due to a periodic arrangement of phase-shifted sources. We will consider a generalised QPG for the case of a one-dimensional array in two-dimensional space. This is obtained by summing phase-shifted singular wavefunctions of the form

$$\mathscr{H}_n(\mathbf{r}) = \mathrm{H}_n^{(1)}(kr)\mathrm{e}^{\mathrm{i}n\theta}, \tag{1}$$

where $\mathrm{H}_n^{(1)}$ represents a Hankel function of the first kind, and θ is the anticlockwise angle between the positive x axis and the vector $\mathbf{r}$. Note the convention that $|\mathbf{r}| = r$ for any vector $\mathbf{r}$, which will be used throughout the paper. Without loss of generality, we assume that the singularities are located on the x axis, with each consecutive pair separated by a distance s_1, so that our generalised QPG takes the form

$$G_n(\mathbf{r}, \beta_x) = \sum_{j=-\infty}^{\infty} \mathrm{e}^{\mathrm{i}js_1\beta_x} \mathscr{H}_n(\mathbf{r} - js_1\hat{\mathbf{x}}), \tag{2}$$

where $\hat{\mathbf{x}}$ is a unit vector in the positive x direction. We have used notation that can be extended to QPGs for two-dimensional lattices because it will be necessary to consider a class of these later. Note that G_n has the quasiperiodicity property

$$G_n(\mathbf{r} + ps_1\hat{\mathbf{x}}, \beta_x) = \mathrm{e}^{\mathrm{i}ps_1\beta_x} G_0(\mathbf{r}, \beta_x), \quad p \in \mathbb{Z}, \tag{3}$$

and the symmetry property

$$G_n(s_1\hat{\mathbf{x}} - \mathbf{r}, \beta_x) = (-1)^n \mathrm{e}^{\mathrm{i}s_1\beta_x} G_n(\mathbf{r}, -\beta_x). \tag{4}$$

Therefore we may restrict attention to the strip in which

$$0 \le x \le s_1/2. \tag{5}$$

The case $n = 0$ corresponds to the classical QPG, except that a source at the point $\mathbf{r} = \mathbf{r}_0$ has the representation $\mathrm{H}_0^{(1)}(k|\mathbf{r} - \mathbf{r}_0|)/(4\mathrm{i})$; we have dispensed with the division by 4i because this factor rarely plays a useful role in applications of QPGs. When $n \neq 0$, we will refer to G_n as a higher order QPG. These are important in situations where the grating elements do not scatter isotropically, and therefore cannot be modelled as points (for a detailed discussion of the circumstances under which such an approximation is valid, see [19]). Higher order QPGs can often be used to efficiently compute the field scattered by a grating or a lattice. For example, if the time-harmonic plane wave

$$U^{\mathrm{i}}(\mathbf{r}, t) = \mathrm{Re}\left[\mathrm{e}^{\mathrm{i}k(x\cos\psi_0 + y\sin\psi_0) - \mathrm{i}\omega t}\right] \tag{6}$$

impinges upon a grating with elements centred at the points $\mathbf{r} = js_1\hat{\mathbf{x}}$, then the scattered field takes the form

$$U^{\mathrm{s}}(\mathbf{r}, t) = \mathrm{Re}\left[\mathrm{e}^{-\mathrm{i}\omega t} \sum_{n=-\infty}^{\infty} A_n \sum_{j=-\infty}^{\infty} G_n(\mathbf{r} - js_1\hat{\mathbf{x}}, k\cos\psi_0)\right]. \tag{7}$$

Here, the wavenumber k is a constant whose relationship to the frequency ω depends on the physical context. For acoustic or electromagnetic waves, $k = \omega/c$, where c is the wavespeed. If we consider waves on the surface of water with depth h, then k

is the positive solution to the dispersion relation $k\tanh(kh) = \omega^2/g$, where g is the acceleration due to gravity [11, chapter 1]. In any case, the coefficients A_n can be determined using the method set out in [13]. At low to moderate frequencies, the sum over n converges very rapidly, so an accurate value for the field at a given point can be computed provided the QPGs in the summand can be evaluated. This approach was used in [24].

Now the series in (2) is not suitable for use in computations, due to the fact that it convergences very slowly, which follows from the large argument asymptotics of the Hankel functions [18, eqn. 10.17.5]. This is a general property of QPGs, and as such, a large body of literature devoted to obtaining rapidly convergent representations in both two and three dimensions now exists; see [16], [10] and references therein. One widely used approach is to convert a QPG into spectral form via Poisson summation. In the particular case of (2) with $n = 0$, the spectral form dates back to [22]. For general n, the spectral representation is given in [24, Appendix A], but in fact it appeared somewhat earlier in a slightly different guise and with a different derivation in [5]. The derivation of the spectral form via Poisson summation was used in [12], though the term QPG was not. The spectral form converges rapidly unless $y \approx 0$, and when $y = 0$ it diverges unless $n = 0$, in which case its convergence properties are no better than those of (2). To address this problem, a number of alternative representations for G_0 were studied in [9]. The most useful of these are the wavefunction expansion (called the 'lattice sum approach' in [9]), which generalises immediately to higher order cases, and the Ewald formula, which does not. The Ewald formula converges very rapidly when $|y|$ is small, and so complete coverage of the (x,y) plane can be achieved using a combination of this and the spectral representation. The wavefunction expansion can be used to further improve efficiency, because it converges more rapidly than the Ewald formula if the observer is close to a source point.

In this paper we construct another representation for G_0 by subtracting unwanted terms from the QPG for an infinite two-dimensional lattice. This idea (i.e. representing a QPG for an n-dimensional lattice in terms of a QPG for an $(n+1)$-dimensional lattice) was used in a similar context in [20]. To perform the subtraction, we require QPGs for parallel rows of sources. Rapidly convergent representations for these were obtained in [23], using a method that originates from [15]. This hinges on the fact that, following Poisson summation in the x direction, the sum of contributions from the rows of sources takes the form of a geometric progression, which can easily be evaluated. To calculate the lattice QPG, we perform Poisson summation in the y direction, so that the sum of contributions from each *column* takes the form of a geometric progression. The resulting formula converges rapidly provided that $x \not\approx 0$, so in conjunction with the standard spectral representation it provides complete coverage of the (x,y) plane, except for the regions close to a source point, where the wavefunction expansion is at its most effective. In contrast to the Ewald formula from [9], the new representation is expressed entirely in terms of elementary functions, and the form of these is such that an arbitrary number of differentiations in both x and y can be applied without difficulty. This allows us to use the idea from [14, section 2.4] to obtain a new representation for G_n from G_0, with minimal effort.

The plan of the paper is as follows. In §2, we summarise the formulae for the spectral and Ewald representations, and the wavefunction expansion. The key formulae

for multirow QPGs from [23] are given in §3. We then show how to obtain the new representation for G_0 in §4, and we compare its computational properties to those of the Ewald formula in §5. In §6, we consider arrays of higher order singularities. Finally, some concluding remarks are made in §7.

2 Known representations for G_0

To obtain the spectral representation for G_0, we require the integral [17, §1.6]

$$\mathrm{H}_0^{(1)}(kr) = -\frac{\mathrm{i}}{\pi}\int_{-\infty}^{\infty} \mathrm{e}^{-\gamma(t)|y|-\mathrm{i}xt}\,\frac{\mathrm{d}t}{\gamma(t)}, \tag{8}$$

where the function γ is given by

$$\gamma(t) = \begin{cases} \sqrt{t^2-k^2} & \text{if } |t| \geq k, \\ -\mathrm{i}\sqrt{k^2-t^2} & \text{if } |t| < k. \end{cases} \tag{9}$$

Substituting (8) into (2) with $n = 0$, we find that

$$G_0(\mathbf{r},\beta_x) = -\frac{\mathrm{i}}{\pi}\sum_{j=-\infty}^{\infty}\int_{-\infty}^{\infty} \mathrm{e}^{-\gamma(t)|y|-\mathrm{i}xt}\mathrm{e}^{\mathrm{i}js_1(\beta_x+t)}\,\frac{\mathrm{d}t}{\gamma(t)}. \tag{10}$$

An application of the Poisson summation formula [7, §9.7] in the form

$$\sum_{j=-\infty}^{\infty}\mathrm{e}^{\mathrm{i}js_1X} = \frac{2\pi}{s_1}\sum_{j=-\infty}^{\infty}\delta(X+2j\pi/s_1) \tag{11}$$

yields

$$G_0(\mathbf{r},\beta_x) = -\frac{2\mathrm{i}}{s_1}\sum_{j=-\infty}^{\infty}\frac{\mathrm{e}^{\mathrm{i}\beta_{xj}x}}{\gamma(\beta_{xj})}\,\mathrm{e}^{-\gamma(\beta_{xj})|y|}, \tag{12}$$

where

$$\beta_{xj} = \beta_x + 2j\pi/s_1. \tag{13}$$

Evidently this series converges rapidly if $|y|$ is large, but the number of terms needed to achieve a useful degree of accuracy can be prohibitive if $y \approx 0$.

The wavefunction expansion for G_0 is obtained by separating the term with $j = 0$ from the remainder of the series in (2) and then using Graf's addition theorem [14, thm. 2.12] to expand the other terms about $r = 0$. For the case in which $n = 0$, the details are given in [9], and the result is that

$$G_0(\mathbf{r},\beta) = \mathrm{H}_0^{(1)}(kr) + \sum_{m=-\infty}^{\infty}(-1)^m\sigma_m(\beta_x)\,\mathscr{J}_m(\mathbf{r}), \quad r < s_1, \tag{14}$$

where the regular wavefunction in the summand is given by

$$\mathscr{J}_m(\mathbf{r}) = \mathrm{J}_m(kr)\mathrm{e}^{\mathrm{i}m\theta}, \tag{15}$$

and the Schlömilch series σ_m is defined as

$$\sigma_m(\beta_x) = \sum_{j=1}^{\infty} \left[\mathrm{e}^{\mathrm{i}js_1\beta_x} + (-1)^m \mathrm{e}^{-\mathrm{i}js_1\beta_x} \right] \mathrm{H}_m^{(1)}(kjs_1). \tag{16}$$

These can be computed using the methods in [10]. As noted in [9], σ_m grows exponentially as $|m|$ increases, but the series in (14) converges if $r < s_1$ because then $\mathscr{J}_m$ decays more rapidly. Indeed, using the large order asymptotics of the Bessel and Hankel functions [18, eqns. 10.19.1–2], we see that

$$\left| \mathrm{J}_m(kr)\, \mathrm{H}_m^{(1)}(kjs_1) \right| \sim \frac{1}{\pi|m|} \left(\frac{r}{|j|s_1} \right)^{|m|} \quad \text{as} \quad |m| \to \infty. \tag{17}$$

In practice, the maximum radius for which (14) can be used is determined by the availability (or otherwise) of routines for accurately computing σ_m at high orders. Typically this maximum radius is much smaller than s_1.

The Ewald formula for G_0, which was also obtained in [9], is given by

$$G_0(\mathbf{r}, \beta_x) = -(S_1 + S_2)/4, \tag{18}$$

where

$$S_1 = \frac{1}{s_1} \sum_{j=-\infty}^{\infty} \frac{\mathrm{e}^{\mathrm{i}\beta_{xj}x}}{\gamma(\beta_{xj})} \left[\mathrm{e}^{\gamma(\beta_{xj})y} \operatorname{erfc}\left(\frac{\gamma(\beta_{xj})s_1}{2\mu} + \frac{\mu y}{s_1} \right) + \mathrm{e}^{-\gamma(\beta_{xj})y} \operatorname{erfc}\left(\frac{\gamma(\beta_{xj})s_1}{2\mu} - \frac{\mu y}{s_1} \right) \right] \tag{19}$$

and

$$S_2 = \frac{1}{\pi} \sum_{j=-\infty}^{\infty} \mathrm{e}^{\mathrm{i}j\beta_x s_1} \sum_{n=0}^{\infty} \frac{1}{n!} \left(\frac{ks_1}{2\mu} \right)^{2n} E_{n+1}\left(\frac{\mu^2 r_j^2}{s_1^2} \right). \tag{20}$$

Here, the exponential integral is given by

$$E_n(t) = \int_1^{\infty} u^{-n} \mathrm{e}^{-ut}\, \mathrm{d}u, \tag{21}$$

and the parameter $\mu \in (0, \infty)$ may be chosen arbitrarily. Increasing μ causes S_2 to converge more rapidly, but slows the rate of convergence of S_1.

3 Green's functions for parallel gratings

The QPG for parallel rows of sources was considered in [23]. Here we construct a slightly less general form, in which the sources are placed on a rectangular grid with consecutive rows separated by a distance s_2; thus

$$G_0^{(q_0,q_1)}(\mathbf{r}, \beta_x, \beta_y) = \sum_{q=q_0}^{q_1} \mathrm{e}^{\mathrm{i}qs_2\beta_y} \sum_{j=-\infty}^{\infty} \mathrm{e}^{\mathrm{i}js_1\beta_x}\, \mathrm{H}_0^{(1)}(k|\mathbf{r} - js_1\hat{\mathbf{x}} - qs_2\hat{\mathbf{y}}|) \tag{22}$$

$$= \sum_{q=q_0}^{q_1} \mathrm{e}^{\mathrm{i}qs_2\beta_y} G_0(\mathbf{r} - qs_2\hat{\mathbf{y}}, \beta_x). \tag{23}$$

After inserting the spectral form for G_0 from (12), the sum over q reduces to a geometric series, provided that $y \leq q_0 s_2$ or $y \geq q_1 s_2$. Evaluating this yields

$$G_0^{(q_0,q_1)}(\mathbf{r},\beta_x,\beta_y) = -\frac{2\mathrm{i}}{s_1}\sum_{j=-\infty}^{\infty}\frac{\mathrm{e}^{\mathrm{i}\beta_{xj}x\mp\gamma(\beta_{xj})y}}{\gamma(\beta_{xj})}\frac{\mathrm{e}^{q_0 w_j^{\pm}}-\mathrm{e}^{(1+q_1)w_j^{\pm}}}{1-\mathrm{e}^{w_j^{\pm}}}, \tag{24}$$

where

$$w_j^{\pm} = s_2\left[\mathrm{i}\beta_y \pm \gamma(\beta_{xj})\right]. \tag{25}$$

Here, β_{xj} is given by (13), and the upper and lower signs are to be taken when $y \geq q_1 s_2$ and $y \leq q_0 s_2$, respectively. It was also noted in [23] that the limits can be extended to infinity, by adding damping to the sources. That is, we write $k = \mathrm{Re}[k] + \mathrm{i}\varepsilon$ where $\varepsilon > 0$, let $q_0 \to -\infty$ or $q_1 \to \infty$, and then take the limit $\varepsilon \to 0$. In this way, we find that

$$G_0^{(q_0,\infty)}(\mathbf{r},\beta_x,\beta_y) = -\frac{2\mathrm{i}}{s_1}\sum_{j=-\infty}^{\infty}\mathrm{e}^{q_0 w_j^{-}}\frac{\mathrm{e}^{\mathrm{i}\beta_{xj}x+\gamma(\beta_{xj})y}}{\gamma(\beta_{xj})\left(1-\mathrm{e}^{w_j^{-}}\right)}, \qquad y \leq q_0 s_2, \tag{26}$$

and

$$G_0^{(-\infty,q_1)}(\mathbf{r},\beta_x,\beta_y) = \frac{2\mathrm{i}}{s_1}\sum_{j=-\infty}^{\infty}\mathrm{e}^{(1+q_1)w_j^{+}}\frac{\mathrm{e}^{\mathrm{i}\beta_{xj}x-\gamma(\beta_{xj})y}}{\gamma(\beta_{xj})\left(1-\mathrm{e}^{w_j^{+}}\right)}, \quad y \geq q_1 s_2. \tag{27}$$

For the full lattice, we may set $q_1 = 0$ and $q_0 = 1$ (or use any other consecutive pair of values) to obtain

$$G_0^{(-\infty,\infty)}(\mathbf{r},\beta_x,\beta_y) = \frac{2\mathrm{i}}{s_1}\sum_{j=-\infty}^{\infty}\frac{\mathrm{e}^{\mathrm{i}\beta_{xj}x}}{\gamma(\beta_{xj})}\left(\frac{\mathrm{e}^{-\gamma(\beta_{xj})y}}{\mathrm{e}^{-w_j^{+}}-1}-\frac{\mathrm{e}^{\gamma(\beta_{xj})y}}{\mathrm{e}^{-w_j^{-}}-1}\right), \quad 0 \leq y \leq s_2. \tag{28}$$

4 New representation for G_0

The first step in obtaining a new representation for the array Green's function is to obtain a representation for the lattice Green's function, with convergence properties different from those of (28). To this end, we observe that we can interchange x and y on the right-hand side of (8) without affecting the value of the integral, which does not depend on θ. We can then apply Poisson summation in the y direction, followed by geometric summation in the x direction. The effect of this is to reproduce the results of §§2 and 3, but with the roles played by x, s_1 and β_x interchanged with those of y, s_2 and β_y, respectively. Hence

$$G_0^{(-\infty,\infty)}(\mathbf{r},\beta_x,\beta_y) = \frac{2\mathrm{i}}{s_2}\sum_{j=-\infty}^{\infty}\frac{\mathrm{e}^{\mathrm{i}\beta_{yj}y}}{\gamma(\beta_{yj})}\left(\frac{\mathrm{e}^{-\gamma(\beta_{yj})x}}{\mathrm{e}^{-u_j^{+}}-1}-\frac{\mathrm{e}^{\gamma(\beta_{yj})x}}{\mathrm{e}^{-u_j^{-}}-1}\right), \quad 0 \leq x \leq s_1, \tag{29}$$

where

$$\beta_{yj} = \beta_y + 2j\pi/s_2 \quad \text{and} \quad u_j^{\pm} = s_1\left[\mathrm{i}\beta_x \pm \gamma(\beta_{yj})\right]. \tag{30}$$

We may now retrieve the Green's function for the array by subtracting unwanted contributions using (26) with $q_0 = 1$ and (27) with $q_1 = -1$; hence

$$G_0(\mathbf{r},\beta_x) = G_0^{(-\infty,\infty)}(\mathbf{r},\beta_x,\beta_y) - G_0^{(1,\infty)}(\mathbf{r},\beta_x,\beta_y) - G_0^{(-\infty,-1)}(\mathbf{r},\beta_x,\beta_y). \tag{31}$$

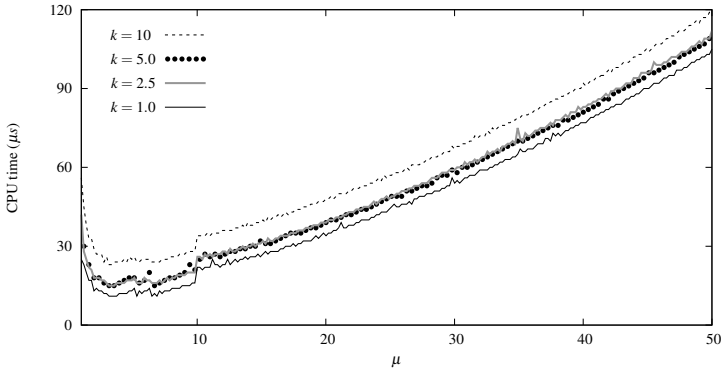

Fig. 1 Computation times for the Ewald formula (18), with $s_1 = 1$, $\beta_x = 1.2$, and $\mathbf{r} = [0.1, 0.01]$.

Here, the first term on the right-hand side must be computed using (29), so that convergence is rapid unless $x \approx 0$ (by symmetry and periodicity we need only consider $x \in [0, s_1/2]$; see §1). If x is close to zero, then we may simply use (12) unless $|y|$ is also small, in which case (14) may be used.

Now the parameters s_2 and β_y do not appear on the left-hand side of (31), so they can be chosen arbitrarily. We choose s_2 to match the rate of exponential decay in the summand of (29) to that of either (26) or (27), whichever is slower. In view of (5), the terms we must consider are $\mathrm{e}^{-\gamma(\beta_{yj})x}$ from (29), and $\mathrm{e}^{\gamma(\beta_{xj})(|y|-s_2)}$, which comes from (26) if $y > 0$ and from (27) if $y < 0$. Letting $|j| \to \infty$ and equating the leading order terms, we find that

$$-\frac{x}{s_2} = \frac{|y| - s_2}{s_1}, \tag{32}$$

which means the correct choice for s_2 is given by

$$s_2 = |y/2| + \sqrt{(y/2)^2 + x s_1}. \tag{33}$$

On the other hand, β_y cannot be used to substantially affect convergence. Instead we use it to avoid the removable singularities in (31), which are caused by the use of two-dimensional QPGs in constructing G_0. Finding the correct value is somewhat involved; this matter is addressed in appendix A.

5 Numerical results

The computational efficiency of the new representation for G_0 (31) was compared to that of the Ewald formula (18), using an implementation written in Fortran 2003 and executed on a machine with a 3.3GHz processor. All summations were truncated at the point where $|t_{n+1}| < \varepsilon |S_n|$, where S_n is the nth partial sum, t_{n+1} is the next term and ε represents machine epsilon (approximately 10^{-16} in double precision). It should be noted that a truly 'fair' comparison is difficult to achieve because (18) requires two special functions, and different algorithms for computing these may lead to different results. In our computations, NAG routines `s15adf` and `s15ddf` are used to evaluate

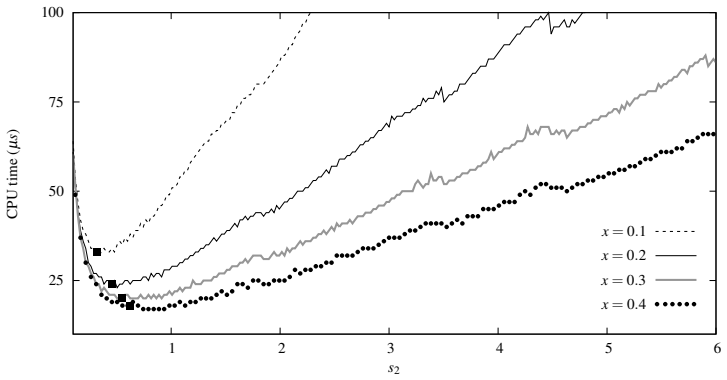

Fig. 2 Computation times for (31), with $s_1 = 1$, $\beta_x = 1.2$, $k = 2.5$ and $\mathbf{r} = [x, 0.01]$. The black squares show the optimal value for s_2 predicted by (33).

complementary error functions, and a Fortran 2003 implementation of the algorithm from [2] is used for the exponential integrals, alongside the recurrence relation

$$nE_{n+1}(t) + tE_n(t) = \mathrm{e}^{-t}. \tag{34}$$

This is numerically stable provided that recurrence is directed away from the integer n which is closest to t [6].

Figure 1 shows the effect of varying the parameter μ on the Ewald formula (18). Results are shown for four different values of k, since this parameter seems to affect the performance of the Ewald formula more strongly than β_x and $\mathbf{r}$. It was noted in [9] that attempting to balance the convergence rates of the series in (18) leads to the value $\mu = \sqrt{\pi}$, but this is an underestimate. Indeed, computations reported in [9] suggest an optimal value in the range $6 \leq \mu \leq 7$, and this is borne out in our results as well. Similarly, figure 2 shows the effect of varying s_2 on the new representation (31). It follows from (29) that the performance of this formula is strongly dependent on x, and so results are shown for four different values of this parameter. The black squares indicate the predicted optimal value for s_2 from (33), and it is clear that this is approximately correct in all four cases.

Finally, figure 3 shows two direct comparisons between the Ewald formula and the new representation. In the case where $x = 0.4$, the Ewald formula is slightly more efficient at low frequencies, whereas the new representation is computed more rapidly for $k \gtrsim 5$. On the other hand, when $x = 0.1$, the Ewald formula performs better, but since $r \approx 0.1$, the wavefunction expansion (14) is the preferred method at this point.

6 Higher order QPGs

A simple way to obtain representations for G_n is to use the operator

$$\mathscr{D} = -\frac{1}{k}\left(\frac{\partial}{\partial x} + \mathrm{i}\frac{\partial}{\partial y}\right), \tag{35}$$

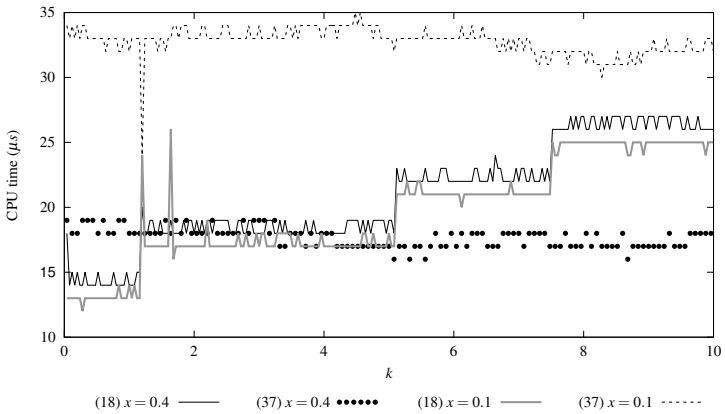

Fig. 3 Comparison between computation times for the Ewald formula (18) and the new representation (31). The parameters used are $s_1 = 1$, $\beta_x = 1.2$ and $\mathbf{r} = [x, 0.01]$. The Ewald parameter is fixed at $\mu = 6$ and the value for s_2 is obtained using (33).

which has the property that [14, §2.4]

$$\mathscr{D}\big[\mathscr{H}_n(\mathbf{r})\big] = \mathscr{H}_{n+1}(\mathbf{r}). \tag{36}$$

Negative indices can be accounted for using the fact that

$$G_{-n}(\mathbf{r}, \beta_x) = (-1)^n G_n(\mathbf{r}_0, \beta_x), \tag{37}$$

where $\mathbf{r}_0 = [x, -y]$. By repeatedly applying the operator $\mathscr{D}$ to (12), we obtain

$$G_n(\mathbf{r}, \beta_x) = \frac{2(-\mathrm{i})^{n+1}}{k^n s_1} \sum_{j=-\infty}^{\infty} \big[\beta_{xj} - (\operatorname{sgn} y)^n \gamma(\beta_{xj})\big]^n \frac{\mathrm{e}^{\mathrm{i}\beta_{xj}x}}{\gamma(\beta_{xj})} \mathrm{e}^{-\gamma(\beta_{xj})|y|}, \quad n = 0, 1, \ldots \tag{38}$$

This representation is not valid if $y = 0$ and $n \neq 0$. The operator $\mathscr{D}$ may also be applied to regular wavefunctions of the form (15) and its effect is the same as in (36). Hence, from (14), we obtain

$$G_n(\mathbf{r}, \beta) = \mathscr{H}_n(\mathbf{r}) + \sum_{m=-\infty}^{\infty} (-1)^m \sigma_m(\beta_x)\, \mathscr{J}_{m+n}(\mathbf{r}), \quad r < s_1. \tag{39}$$

Note that this can also be obtained directly by applying the method from [9] to (2) without first setting $n = 0$. The *mismatch* in the indices for the wavefunction and the Schlömilch series slows down convergence as $m \to -\infty$. For large n, (39) should only be used in cases where $r \ll s_1$. Finally, we find that (31) generalises to yield

$$G_n(\mathbf{r}, \beta_x) = G_n^{(-\infty,\infty)}(\mathbf{r}, \beta_x, \beta_y) - G_n^{(1,\infty)}(\mathbf{r}, \beta_x, \beta_y) - G_n^{(-\infty,-1)}(\mathbf{r}, \beta_x, \beta_y), \tag{40}$$

where

$$G_n^{(-\infty,\infty)}(\mathbf{r},\beta_x,\beta_y)=\frac{2\mathrm{i}}{s_2k^n}\sum_{j=-\infty}^{\infty}\frac{\mathrm{e}^{\mathrm{i}\beta_{yj}y}}{\gamma(\beta_{yj})}\left(\frac{\left[\beta_{yj}+\gamma(\beta_{yj})\right]^n}{(\mathrm{e}^{-u_j^+}-1)\mathrm{e}^{\gamma(\beta_{yj})x}}-\frac{\left[\beta_{yj}-\gamma(\beta_{yj})\right]^n}{(\mathrm{e}^{-u_j^-}-1)\mathrm{e}^{-\gamma(\beta_{yj})x}}\right), \tag{41}$$

$$G_n^{(1,\infty)}(\mathbf{r},\beta_x,\beta_y)=\frac{2(-\mathrm{i})^{n+1}}{s_1k^n}\sum_{j=-\infty}^{\infty}\left[\beta_{xj}+\gamma(\beta_{xj})\right]^n\frac{\mathrm{e}^{\mathrm{i}\beta_{xj}x+\gamma(\beta_{xj})y}}{\gamma(\beta_{xj})\left(\mathrm{e}^{-w_j^-}-1\right)} \tag{42}$$

and

$$G_n^{(-\infty,-1)}(\mathbf{r},\beta_x,\beta_y)=\frac{2(-\mathrm{i})^{n+1}}{s_1k^n}\sum_{j=-\infty}^{\infty}\left[\beta_{xj}-\gamma(\beta_{xj})\right]^n\frac{\mathrm{e}^{\mathrm{i}\beta_{xj}x-\gamma(\beta_{xj})y}}{\gamma(\beta_{xj})\left(\mathrm{e}^{w_j^+}-1\right)}. \tag{43}$$

The optimal values for s_2 and β_y used in computing (31) (see (33) and appendix A) should also be used in these formulae.

7 Conclusions

We have derived a new representation for the quasiperiodic Green's function corresponding to an array of sources, intended for use when the observer is located close to, or on, the axis of the array. At such locations, the standard spectral representation converges very slowly. An earlier attempt to address the same problem was made using Ewald summation in [9], and we have compared the properties of the two approaches. The new representation is expressed purely in terms of elementary functions, so it is somewhat simpler to compute than the Ewald formula, which involves special functions. Both formulae can be computed accurately and efficiently. Our numerical experiments favour the new representation, but only slightly. The Ewald formula is slightly more efficient if the observer is close to a source, but this is precisely the region in which the wavefunction expansion (14) is the best method. The new representation is easily generalised to cases involving arrays of higher order singularities. Whilst it is possible to extend the Ewald formula in this way, the result is much more complicated.

A The parameter β_y

Viewed as a function of β_y, the representation (29) has removable singularities (RSs) at points where $\gamma(\beta_{yj})=0$ for some $j\in\mathbb{Z}$, and also at points where $\mathrm{i}s_1\beta_x\pm s_1\gamma(\beta_{yj})=2p\pi\mathrm{i}$ for integers j and p. Thus, an RS occurs when either

$$(\beta_y+2j\pi/s_2)^2=k^2 \tag{A1}$$

or

$$(\beta_x+2p\pi/s_1)^2+(\beta_y+2j\pi/s_2)^2=k^2 \tag{A2}$$

can be solved exactly using integers j and p. In general, none of these correspond to actual singularities of G_0, and we aim to choose β_y in such a way that the distance to the nearest RS is maximised. We need only consider values such that $|\beta_y|\le\pi/s_2$ since larger values represent periodic repetitions. Moreover, the RSs are symmetric about $\beta_y=0$, so nothing is gained by allowing negative values. Points where

$(\beta_x + 2p\pi/s_1)^2 = k^2$ has an integer solution for p are actual singularities of G_0 (see §1). We are not concerned with these here.

For (A1), we have

$$\left| \frac{\beta_y s_2}{2\pi} + j \right| = \alpha \tag{A3}$$

where we have written

$$\alpha = k s_2/(2\pi). \tag{A4}$$

Since $0 \le \beta_y s_2 \le \pi$, we find that

$$\beta_y = \begin{cases} \dfrac{2\pi}{s_2}\big(\alpha - \lfloor \alpha \rfloor\big) & \text{if } \alpha - \lfloor \alpha \rfloor \le \dfrac{1}{2} \\ \dfrac{2\pi}{s_2}\big(\lfloor \alpha + 1 \rfloor - \alpha\big) & \text{if } \alpha - \lfloor \alpha \rfloor > \dfrac{1}{2}, \end{cases} \tag{A5}$$

where $\lfloor \cdot \rfloor$ indicates rounding toward $-\infty$.

For (A2), we begin by noting that the minimum and maximum values for p such that real solutions are possible are given by

$$p_{\min} = \left\lceil -\frac{s_1}{2\pi}(k + \beta_x) \right\rceil \quad \text{and} \quad p_{\max} = \left\lfloor \frac{s_1}{2\pi}(k - \beta_x) \right\rfloor, \tag{A6}$$

where $\lceil \cdot \rceil$ indicates rounding toward infinity. Rearranging (A2), we obtain

$$\left| \frac{\beta_y s_2}{2\pi} + j \right| = \frac{s_2 \Delta(p)}{2\pi}, \tag{A7}$$

where

$$\Delta(p) = \sqrt{k^2 - (\beta_x + 2p\pi/s_1)^2}. \tag{A8}$$

Solutions are therefore given by (A5), with k replaced by $\Delta(p)$ in (A4).

To select a value for β_y, we arrange the values that allow integer solutions to either (A1) or (A2) in ascending order, and denote these by $r_1, \ldots, r_n$, say. By periodicity and symmetry, the next RS occurs at $r_{n+1} = 2\pi/s_2 - r_n$, so if we ultimately choose β_y such that $\beta_y > r_n$ then the distance to the closest RS is $\beta_y - r_n$. We do not use a similar argument at the left-hand end of the interval, because the solutions to (A2) with $j = 0$ and $p = p_{\min} - 1$ or $p = p_{\max} + 1$ may lie close to the origin on the imaginary axis. To safely neglect these, we set $r_0 = 0$. Finally, we find the natural number $m \le n + 1$ which maximises $r_m - r_{m-1}$, and choose $\beta_y = (r_m + r_{m-1})/2$.

References

1. Abawi, A.T.: The use of the virtual source technique in computing scattering from periodic ocean surfaces. J. Acoust. Soc. Am. **130**(2), 683–688 (2011).
2. Amos, D.E.: Computation of exponential integrals. ACM Trans. Math. Software **6**(3), 365–377 (1980)
3. Ayaz, Y., Akinci, N.: Dyadic green's function study of band structures of dispersive photonic crystals. Journal of Quantitative Spectroscopy and Radiative Transfer **112**(18), 2814–2825 (2011).
4. Bennetts, L.G., Squire, V.A.: Linear wave forcing of an array of axisymmetric ice floes. IMA J. Appl. Math. **75**(1), 108–138 (2010).
5. Botten, L.C., Nicorovici, N.A., Asatryan, A.A., McPhedran, R.C., de Sterke, C.M., Robinson, P.A.: Formulation for electromagnetic scattering and propagation through grating stacks of metallic and dielectric cylinders for photonic crystal calculations. Part I. Method. J. Opt. Soc. Am., A **17**, 2165–2176 (2000)
6. Gautschi, W.: Recursive computation of certain integrals. J. ACM **8**, 21–40 (1961).
7. Jones, D.S.: The Theory of Electromagnetism. International Series of Monographs in Pure and Applied Mathematics. Pergamon Press, Oxford (1964)
8. Linton, C., McIver, M.: Periodic structures in waveguides. Proc. Roy. Soc. Lond., A **458**, 3003–3021 (2002)

9. Linton, C.M.: The Green's function for the two-dimensional Helmholtz equation in periodic domains. J. Engng. Math. **33**, 377–402 (1998)
10. Linton, C.M.: Lattice sums for the Helmholtz equation. SIAM Review **52**(4), 630–674 (2010)
11. Linton, C.M., McIver, P.: Handbook of Mathematical Techniques for Wave/Structure Interactions. Chapman & Hall/CRC, Boca Raton (2001)
12. Linton, C.M., Thompson, I.: Resonant effects in scattering by periodic arrays. Wave Motion **44**, 167–175 (2007)
13. Maniar, H.D., Newman, J.N.: Wave diffraction by a long array of cylinders. J. Fluid Mech. **339**, 309–330 (1997)
14. Martin, P.A.: Multiple Scattering. Interaction of Time-Harmonic Waves with *N* Obstacles. Cambridge University Press (2006)
15. McPhedran, R.C., Nicorovici, N.A., Botten, L.C., Grubits, K.A.: Lattice sums for gratings and arrays. J. Math. Phys. **41**(11), 7808–7816 (2000)
16. Moroz, A.: Quasi-periodic Green's functions of the Helmholtz and Laplace equations. J. Phys. A **39**, 11,247–11,282 (2006)
17. Noble, B.: Methods Based on the Wiener–Hopf Technique. Chelsea (1988)
18. Olver, F.W.J., Lozier, D.W., Boisvert, R.F., Clark, C.W.: NIST Handbook of Mathematical Functions. Cambridge University Press (2010)
19. Parnell, W.J., Abrahams, I.D.: Multiple point scattering to determine the effective wavenumber and effective material properties of an inhomogeneous slab. Waves in Random and Complex Media **20**, 678–701 (2010)
20. Silveirinha, M.G., Fernandes, C.A.: A new acceleration technique with exponential convergence rate to evaluate periodic Green functions. IEEE Trans. Antennas Propagat. **53**(1), 347–355 (2005)
21. Smith, M.J.A., Meylan, M.H., McPhedran, R.C.: Flexural wave filtering and platonic polarisers in thin elastic plates. Q. J. Mech. Appl. Math. **66**(4), 437–463 (2013).
22. Twersky, V.: On the scattering of waves by an infinite grating. IRE Trans. on Antennas and Propagation **4**, 330–345 (1956)
23. Tymis, N., Thompson, I.: Low-frequency scattering by a semi-infinite lattice of cylinders. Q. J. Mech. Appl. Math. **64**(2), 171–195 (2011)
24. Tymis, N., Thompson, I.: Scattering by a semi-infinite lattice of cylinders and the excitation of Bloch waves. Q. J. Mech. Appl. Math. **67**(3), 469–503 (2014).